Electric Power Systems Research 147 (2017) 165–173

Contents lists available at ScienceDirect

Electric Power Systems Research

journal homepage: www.elsevier.com/locate/epsr

A holistic approach to power quality parameter optimization in AC coupling Off-Grid systems

Stanislav Misak, Jindrich Stuchly*, Tomas Vantuch, Tomas Burianek, David Seidl, Lukas Prokop

Centre ENET, VSB- TU Ostrava, 15 17. listopadu, Ostrava, Czechia

ARTICLE INFO

Article history:
Received 9 July 2016
Received in revised form 25 January 2017
Accepted 21 February 2017

Keywords:
Off-Grid system
Power quality
Renewable energy sources
Artificial intelligence

ABSTRACT

The development of autonomous energy systems has been accompanied by a number of challenges related to the specific characteristics of these systems, such as power flow control, development of protection systems respecting the dynamic changes in short-circuit power and the issue of compliance with power quality parameters. To keep the power quality parameters of electrical energy in Off-Grid systems within the limit is highly complicated with regards to the supply of electrical energy from renewable sources of a stochastic nature, which are used as dominant sources of electric or heat energy. Variations in short-circuit power may significantly affect the system stability and may have a negative impact on the operation in case of sensitive appliances. We developed tools and methods to keep the power quality parameters in Off-Grid systems within the limits using an intelligent approach based on an artificial intelligence technique. Our computational model is able to predict disturbances in power quality and perform a set of proper reactions to avoid such disturbances with over 60% success rate in time horizon of 15 min ahead. As a result, it is subsequently possible to optimize the operation of Off-Grid systems and thus contribute to improvements in the power quality parameters in Off-Grid systems.

1. Introduction

Autonomous energy systems (also Off-Grid systems) are often operated in conjunction with Renewable Energy Sources (RES), such as Wind Power Plants (WPP), Photovoltaic Power Plants (PV), liquefied petroleum gas (LPG) generators, etc. to generate electricity. The development of energy storage systems and sophisticated control algorithms allows a reliable and affordable electricity generation using RES in year-round operation [1–3].

However, some fundamental difficulties associated with the Off-Grid systems are the issues of power flow control (including appliance prioritization), further developments in protection relay concepts, and the issue of power quality (PQ) parameters. One of the key technical issues to be solved in relation to the operation of the Off-Grid system is to keep the PQ parameters of electric energy system within the limits [4–6].

In general, the PQ parameters can be defined as values of voltage, power frequency, total harmonic distortion of voltage and current, short-term and long-term flicker severity, etc [4,7]. If the PQ parameters are not in the allowed limits, this may lead to reductions in the efficiency of electrical appliances or even cause irreversible damage in sensitive appliances. To keep the PQ parameters of electrical energy in the Off-Grid systems within the limit is extremely difficult when electrical energy is supplied from RES. These are usually stochastic in nature, which implies fluctuations in PQ in the Off-Grid systems [8,9,15]. This problem can be solved by using energy storage devices, plug-in vehicles or sophisticated management systems (demand side management) able to ensure the supply of electric energy for all operating modes [10–14].

The major problem that affects the quality of electric power, or more precisely the PQ parameters, is the value of short-circuit power. The short-circuit power in the Off-Grid system is usually several times lower than that in the conventional On-Grid systems, and the value changes during various operating modes of a power converter [16–19].

With regard to the results of the currently published research, the studies usually concentrate on a narrow aspect of the phenomenon of PQ controlling [20–24]. The method presented in Ref. [20] solves the PQ in an autonomous wind/diesel power system using an intelligent adaptive system, but does not mention any potential lack of energy in time, and regulates the PQ in the Off-Grid using power controllers. Different methods presented in Refs. [21]

* Corresponding author.
E-mail address: jindrich.stuchly@vsb.cz (J. Stuchly).

http://dx.doi.org/10.1016/j.epsr.2017.02.021
0378-7796/

and [22] quantify and measure the PQ parameters or try to find optimized allocations of power quality monitors in the transmission systems [23], however only in the On-Grid system. The research reviewed in Ref. [24] optimizes only some of the components of the Off-Grid system with regard to PQ parameters.

Some artificial intelligence methods are useful in forecasting PQ parameters, such as those presented in Refs. [25–28]. Such methods gained a lot of attention also in other fields of study [29,30], which confirms their relevancy of application. However, based on the available literature, these methods have not been verified for the Off-Grid systems to date, and the PQ parameter forecasts have been done for one PQ parameter only.

The reviews in Refs. [31,32] conclude that most of the PQ disturbance classification models are based on online detection and moderation of the problem instead of their avoidance in the first place. Our approach focuses mainly on developing new methods and tools to keep the PQ parameters in allowed limits and their real implementation in Active Demand Side Management (ADSM) [1] of the Off-Grid system. This makes it different from the available research reviews in this field. Such advantage is achieved by forecasting disturbances and applying an active management of electric energy demand.

The optimization of the PQ parameters supported by artificial intelligence methods in Off-Grid systems can be considered a huge challenge. This research paper presents a novel approach to PQ parameter optimization (PQPO), which allows a comprehensive optimization of the Off-Grid system operation using AC coupling topology. This optimization is grounded in a PQ parameter forecasting tool using artificial intelligence (support vector regression) and a subsequent feedback optimization process to keep the PQ parameters within allowable limits in all operating modes, while an optimized operation of the Off-Grid system is guaranteed. The complex approach described in this paper ties together artificial intelligence forecasting with autonomous feedback control on hardware platform, which makes us able to evaluate the validity of the entire ADSM model for the first time ever. The optimization tool for PQ parameters works as an integral part of ADSM for Off-Grid systems presented in Ref. [1] — see details of the tested experimental platform in Fig. 1.

2. Description of the experimental platform

In 2011, an experimental platform operating in an Off-Grid mode was developed in the campus of VSB — Technical University of Ostrava, Czech Republic, see Fig. 1. Its main purpose is to simulate household conditions via applying the most common household appliances. This platform comprises of all specific Off-Grid System requirements, namely:

- Autonomous operation independent of energy from external power grids.
- Equable generation–consumption balance.
- Possibility of energy storage.
- Predominant use of RES.
- Capability to serve non-traditional loads.
- New type of a relay protection concept allowing for bi-directional power flows and short-circuit power changes [19].
- Active Demand Side Management [1].

A detailed description of the proposed Off-Grid system can be found in Refs. [1] and [19].

The tested Off-Grid experimental platform is supplied by a PV system with a battery bank functioning as a storage device. The PV is divided into 2 strings (PV_1 and PV_2 in Fig. 1), and the maximum installed power of each string is 2 kWp. The battery bank uses Ni–Cd batteries with an installed capacity of 750 A·h at the 24 V level on the DC bus-bar.

The heart of the Off-Grid system is a hybrid inverter (SI in Fig. 1). This inverter creates the standard single phase AC grid (230 V/50 Hz) with adjustable grid parameters, e.g. voltage,

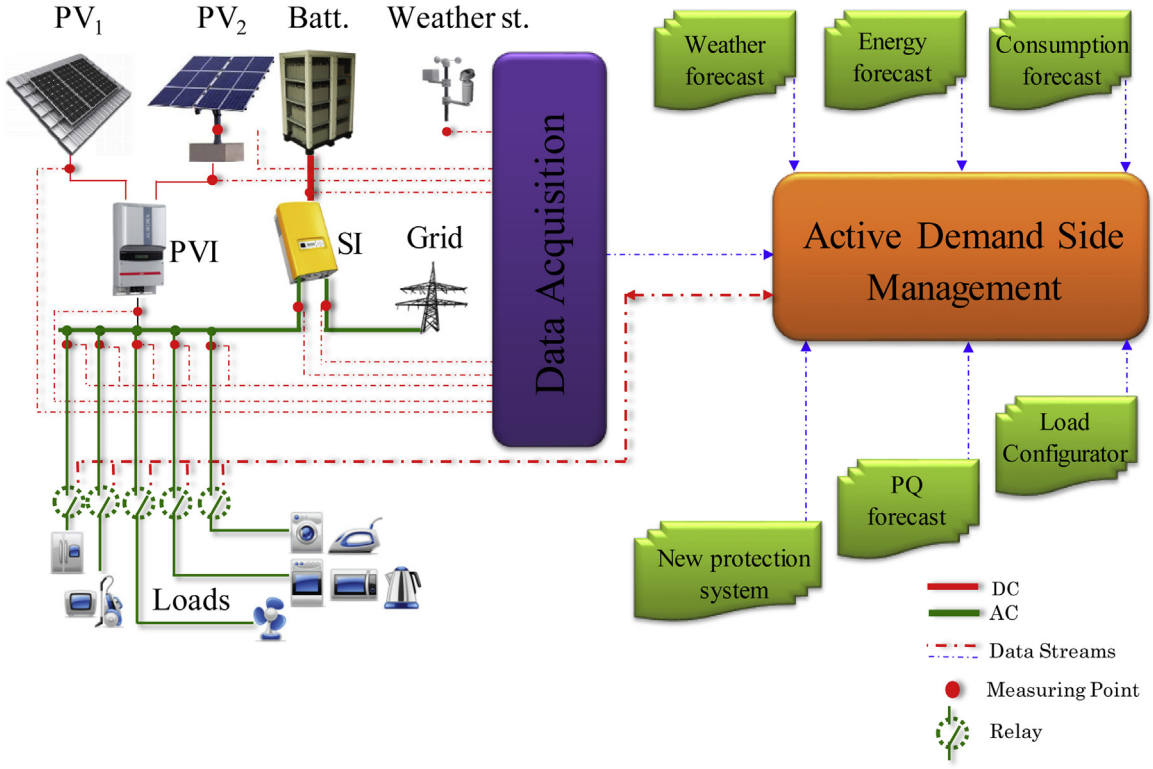

Fig. 1. Experimental platform of the Off-Grid system.

Table 1
Loads used in the experimental platform.

Household appliance	Power input (W)	Household appliance	Power input (W)
LCD Screen 24″	25	Microwave oven	1160
Notebook + dock station	50	Kettle	960
Stereo speakers	10	Refrigerator	150
Colour laser printer	1050	LCD TV 32″	110
AC/heating	1400/2000	Hot water heating	550
Solar collector accessories	80	Programmable load	0–4000

power frequency, maximal loads, etc. The hybrid inverter is a bi-directional battery power converter (battery inverter and charger) and it supports the use of power sources on AC side (generator, low-voltage external grid — GRID in Fig. 1, photovoltaic inverter — PVI in Fig. 1) [33].

Electricity consumption in the Off-Grid system significantly affects the parameters of the installed power sources and the PQ parameters of electric energy. The electrical appliances used in the experimental platform are listed in Table 1.

3. Data processing and variables dependency extraction

3.1. Data acquisition

As data inputs for the developed forecasting models, we created a large database of 118 variables of one minute measurements during the entire year (2015), so it contained conditions of the Off-Grid for all seasons. To describe the weather conditions observed and measured in the area where the laboratory is placed, we made Table 2 evaluating the typical days for each season through relevant variables. Each typical day represents the day whose highest level and overall progress of solar irradiance was the closest to the median of these values of its season. The average values of the weather conditions and energy generation consumption were calculated on such days. P1_avg is the active power consumption of the Off-Grid system, S1_avg is the apparent power consumption of the Off-Grid system, and S_SI is the apparent power delivered to the Off-Grid system by the Off-Grid converter – marked as SI in Fig. 1.

The complete database (created from the detailed monitoring system) contains variables describing the weather conditions, such as wind direction, air temperature, relative humidity, etc. Next, there are the power consumption and generation parameters — active, reactive, apparent powers or power factors of individual converters, battery bank parameters, PV array, PQ parameters, etc. However, not all the variables from the given dataset are relevant for the forecasting model. The selected weather parameters and their relevancy confirmed by estimation of mutual information (MI) are depicted in Fig. 2.

The output values from the forecasting models were predictions of PQ parameters, such as the value of long term flicker severity (*Plt*) — calculated from the short-term flicker severity (*Pst*), total harmonic distortion of voltage (*THDu*), total harmonic distortion of current (*THDi*) and power frequency (*freq*). All these values are predicted in time from 1 to 4 ticks ahead.

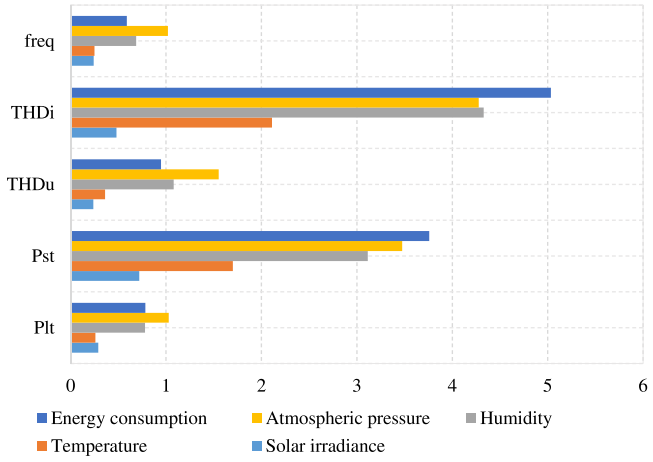

Fig. 2. Diagram of the computed relevancy by mutual information for parameters with non-zero dependency.

3.2. Variables' relevancy estimation

The nature of the applied algorithms lies in the self-handling of relevant and irrelevant variables via modification of (input) weights during the learning time. A larger amount of the applied variables may increase the duration of the learning process and may lead to finding a local, instead of global, optimum. This phenomenon may decrease the total performance [34].

For this reason, to pick the most suitable subset for each of the predicted variables, we performed several evaluations of input variable relevancy to the predicted PQ parameters. Although the physical dependencies were known and clearly defined, the applied measuring procedure could have potentially decreased this relevancy in the averaged values of the used time frames.

Table 2
Average values of parameters in typical days of the seasons.

Parameter	Winter		Spring		Summer		Autumn	
Max. solar irradiance ($W \cdot m^{-2}$)	266.7		715.6		885.2		498.9	
Hours of sunlight	7.5		12.1		14.2		10.6	
	[a]	[b]	[a]	[b]	[a]	[b]	[a]	[b]
Wind speed ($m \cdot s^{-1}$)	3.3	3.4	1.1	1.7	2.1	2.4	0.2	0.5
Temperature (°C)	4.6	5.1	12.3	15.6	21.1	22.7	13.3	16.4
Pressure (hPa)	981	983	978	978	982	983	984	981
P1_avg (W)	170	219	63	89	851	1164	225	306
S_SI (V·A)	757	759	504	464	649	685	429	458
S1_avg (V·A)	1041	1067	261	153	944	1242	366	397

[a] Total average in selected session of the year 2015.
[b] Daily average in selected session of the year 2015.

The first dependency measure was the familiarly known correlation coefficient [35]. This measure is simple to estimate, but on the other hand, it only reflects a linearly based dependency.

Another applied analysis was the evaluation of causal interactions, especially the computing of Granger causalities [36]. This staetctistical measure, in our case, does not reveal any significant direct causal relations inside the given data set.

The relevancy measurement, which was applied with success, was the MI calculated by Kraskov estimation [37]. This multivariate approach is able to evaluate the relevancy of each of the variables and the total relevancy of the selected subset. Kraskov estimation is based on Kozachenko–Leonenko entropy estimation (Eq. (1)) [37]:

$$\hat{H}(X) = -\psi(K) + \psi(N) + \log(c_d) + \frac{d}{N}\sum_{n=1}^{N} log(\varepsilon_X(N,K)) \quad (1)$$

where N means the number of samples in X, d is the dimensionality of samples x, c_d means the volume of a d-dimensional unitary ball, and $\varepsilon_X(N,K)$ is twice the distance (usually chosen as the Euclidean distance) from x_i to its k-th neighbour. The most known derivate of MI estimation has the following form (Eq. (2)) [37]:

$$\hat{I}(X;Y) = \psi(\mathrm{N}) + \psi(\mathrm{K}) - \frac{1}{K} - \frac{1}{N}\sum_{i=1}^{N}\left(\psi\left(\tau_{x_i}\right) - \psi\left(\tau_{y_i}\right)\right) \quad (2)$$

where τ_{x_i} is the number of points whose distance from x_i is not greater than $0.5 * \varepsilon_X(i) = 0.5 * \max(\varepsilon_X(i), \varepsilon_Y(i))$. As we can see, the Kraskov's MI does not require the computation of underlying probability distributions of the given time series, but simply estimates the dependency by its K-NN clustering. This simplifies the entire approach. A comparative review by Doquire and Verleysen confirmed its performance against other widely known estimation approaches [38]. MI estimated by this approach was also the backbone of the feature selection in several studies [39,40].

The estimated MI does not reflect how a modification of one variable affects the progress of another, and this task is solved herein by applying a machine learning model. The relevancy of the mentioned variables to the predicted parameters is depicted in Fig. 2. This computation was performed with a time shift of 1 tick backwards according to the predicted variable, so we computed how relevant the averaged value of the previous minute was to the one minute's future value of the predicted PQ parameter.

3.3. Power generation forecasting

One of the key parts of the ADSM concept is the module responsible for the forecast of generated energy by photovoltaic panels. The knowledge about the amount of energy available in the future is one of the most relevant pieces of information during the optimization of an energy consumption plan. This prediction also enables us to compute the amount of energy to be available in batteries in the future, and therefore this variable can be applied as an input in PQ forecasting without time-shifting, which increases the performance of the PQ forecasting model.

The applied data for power generation prediction was obtained from meteorological forecasts. In hourly time frames they describe the progress of variables, such as air temperature, humidity, wind speed, cloudiness and atmospheric pressure. Cloudiness and maximum solar irradiation were considered the most relevant parameters for this experiment. In order to improve the performance of the model we computed the maximum solar irradiation for a particular hour, which was performed by interpolation over all the sunny days in the year. The final forecasting of power generation was made using the Recurrent Neural Network with the backpropagation through time learning algorithm. Details about the algorithm, the input variables, the adjustment of the predictive model and results are given in our previous paper [41].

4. PQ forecasting — support vector regression application

Support vector regression (SVR) was applied as the backbone of the predictive model in PQPs' values. SVR as a robust regression technique with an alternative loss function originates from the Support Vector Machine (SVM) algorithm proposed by Vapnik [42]. Since then it has been a very frequently applied regression model [43,44]. The advantages of SVR lies in possible handling of over-fitting by adjusting its penalization constant and in the ability to apply expert knowledge by proper selection of kernel function. The correctly applied kernel function brings a nonlinear solution with a still very fast and effective computational effort when compared to the Artificial Neural Network or Ensemble based models. A good generalization performance of the model is supported by a convex optimization that implies the sparseness of the solution with the absence of local minima. The regression, in general, creates an approximation function $y = f(x)$ that returns the value y as the prediction of target values d according to the given dataset $G = \left\{(x_i, d_i)\right\}^n$, where x_i denotes the vector of input variables and d_i represents the predicted value in all the given n observations.

We should start by pointing at the generic equation of SVR's estimation below (Eq. (3)) [42]:

$$f(x) = (w \cdot \Phi(x)) + b \quad (3)$$

where w represents a weight vector and b is the coefficient of the regression. $(w \cdot \Phi(x))$ is the dot production in the feature space **F** and Φ is the kernel function that performs nonlinear mapping of input vectors to a higher dimensional feature space. This mapping turns the entire algorithm into nonlinear regression, even if the regression in high-dimensional feature space can be purely linear. The core of the algorithm is the regularized risk function that is an objective for optimization of w and b, and its form is meant to increase the generalization capability and prevent over-fitting of the solution:

$$R(C) = C\frac{1}{n}\sum_{i=1}^{n} L_\varepsilon(d_i, y_i) + \frac{1}{2}|w|^2 \quad (4)$$

where L_ε is applied ε-intensive loss function described bellow:

$$L_\varepsilon(f(x), q) = \begin{cases} |f(x) - q| - \varepsilon; |f(x) - q| \geq \varepsilon \\ 0; otherwise \end{cases} \quad (5)$$

The formula $|w|^2/2$ denotes the Euclidean norm. The minimization of vector w increases the flatness of $f(x)$, which implies a higher generalization of the solution. C is the penalization constant of the cost function to evaluate the empirical risk. It evaluates the penalty of the fitting error when it exceeds the radius according to the ε-intensive loss function $L_\varepsilon(f(x), q)$, which stabilizes the estimation. This trade-off is also able to reduce noise in the model. All the points with non-zero value are considered as support vectors and they are represented by slacked variables ξ_i, ξ_i^*, which transforms the minimization problem into the following formula (Eq. (6)):

$$\text{Minimize}: R_{reg}(f) = C\sum_{i=1}^{n}\left(\xi_i + \xi_i^*\right) + \frac{1}{2}|w|^2 \quad (6)$$

$$\text{Subject to}: \begin{cases} q_i - (w \cdot \Phi(x)) - b \leq \varepsilon + \xi_i \\ -q_i + (w \cdot \Phi(x)) + b \leq \varepsilon + \xi_i^* \\ \xi_i, \xi_i^* \geq 0, \text{for} i = 1, \ldots, n \end{cases} \quad (7)$$

Such constrained optimization can be solved by applying Lagrange multipliers $L_d(\alpha,\alpha^*)$, which was also outlined by Vapnik and Vapnik [42]. The vector w can be rewritten under this assumption to the following equation:

$$\text{Minimize}: L_d(\alpha, \alpha^*) = -\varepsilon \sum_{i=1}^{n} \left(\alpha_i - \alpha_i^*\right) + \sum_{i=1}^{n} \left(\alpha_i - \alpha_i^*\right) q_i - \frac{1}{2} \sum_{i,j=1}^{n} \left(\alpha_i - \alpha_i^*\right) \left(\alpha_j - \alpha_j^*\right) K\left(x_i, x_j\right) \quad (8)$$

$$\text{Subjected to}: \begin{cases} \sum_{i=1}^{n} \left(\alpha_i - \alpha_i^*\right) = 0 \\ 0 \le \alpha_i \le C, i = 1, \ldots, n \\ 0 \le \alpha_i^* \le C, i = 1, \ldots, n \end{cases} \quad (9)$$

Calculating the Lagrange multipliers, the desired weight vector is, $w = \sum_{i,j=1}^{n} \left(\alpha_i - \alpha_i^*\right) K\left(x_i, x_j\right)$ and substituting the generic equation, we obtain the formula below:

$$f(x, w) = f(x, \alpha, \alpha^*) = \sum_{i=1}^{l} \left(\alpha_i - \alpha_i^*\right) K(x_i, x) + b \quad (10)$$

where n is the number of support vectors and K denotes the previously mentioned kernel function. The Lagrange multipliers represent the solution of the quadratic problem and it forces the forecasting towards the target value. The Lagrange multipliers obtain a zero value for all the points positioned inside the ε–tube (Eq. (9)). The points with non-zero values are actually more useful to estimate the position of the regression line and they are considered support vectors.

Modifying the penalization constant C, we can control the generalization capability of the model. In case of higher C, a higher penalization forces the optimization to create a more specific solution with a lower generalization although a lower C value brings more generalization with lower specificity. In solving the value of b, we can apply the Karush–Kuhn–Tucker (KKT) conditions [45].

The user's adjustable parameters are the kernel function, the penalization constant C and the radius ε. Some of the kernel functions bring additional parameters, such as the gamma value in case of the radial basis function or sigmoidal function. In many studies, those constants are set experimentally or tuned in order to obtain the best possible performance based on some fundamental knowledge of the dataset. In our study, we applied Hyper-parameter optimization by Particle Swarm Optimization to find the best combination of parameter adjustment. Running multiple evaluations of the machine learning model inside the optimization required the application of a computational learning model capable of a high convergence, which SVR certainly is.

4.1. Hyper-parameter optimization by Particle Swarm Optimization

The adjustment of the previously defined parameters was optimised by Particle Swarm Optimization (PSO) algorithm, which had been inspired by a study of Yassi and Moattar, where PSO is applied for SVM parameter estimation [46]. PSO is a bio-inspired search optimization approach [45]. This algorithm processes each defined constant as a dimension of the searched space. In this space, there are agents (particles of a swarm) randomly distributed and their positions are evaluated according to the performance of the model. Such evaluation is supported by a given fitness function. In this experiment, each particle i was evaluated by a fitness value computed as the average of RMSE (Section 4.2) values from Cross-validation testing of the SVR model, the adjustment parameters of which were obtained from particle's position vector x_i.

The algorithm runs in iterations and a leader (particle with the best position) has to be selected during each of them. Subsequently, all the other particles attempt to reach the leader's position by moving over the searched space, which is driven by adjusted velocity and direction (towards the leader or personal optimum). The following formulas (Eqs. (9), (10)) describe an update of the particle's position [45].

$$v_{i,d} = \omega v_{i,d} + \varphi_p r_p \left(p_{i,d} - x_{i,d}\right) + \varphi_g r_g \left(g_d - x_{i,d}\right) \quad (11)$$

$$x_i = x_i + v_{i,d} \quad (12)$$

where p denotes particle's personal best position and g denotes the position of the leader (global best position). The letter x represents particle's actual position, φ brings weight to the consideration of personal or global position respectively, and ω serves as inertia for previous velocity v.

During the defined number of iterations, particles find the adjustment that is close to the ideal solution. Table 3 describes the optimized parameters and their pre-defined values or value ranges. Each dimension of the particle's definition was therefore normalized between values 0 and 1, and during the evaluation of the fitness function the proper mapping was applied according the parameter's value. The fitness function of the mentioned particles was based on the testing performed by Cross-validation (CV) [46]. This process splits the data set into five smaller blocks, where each block is subsequently split into training and testing subsets. The performance of these five different tests was averaged. This operation brings more stable results over the complete data set with a decrease of over-fitting. The adjustment with the highest performance as a winning combination was taken as the result of the fine-tuned regression model. The hyper-parameters of PSO were adjusted experimentally according to previous studies [47] (see Table 4).

The final adjustments of the models differed in the predicted PQPs and duration of the prediction. The radial basis function was the winning kernel function in all the models and the value of radius was mostly close to 0.1.

Table 3
Optimized parameters and their pre-defined values or ranges of values.

Parameters	Value
Penalization constant (C)	[1100]
Kernel function	Linear (lin), polynomial (poly), radial basis (rbf), sigmoid (sig)
Radius (ε)	[0.001, 1]
Gamma (parameter for kernel functions, such as poly, rbf, sig)	[0.01, 100]

Table 4
Adjustment of PSO's attributes.

Parameters	Value
Number of particles	25
Number of iterations	1000
Max position	1
Min position	0
Velocity	0.05
Threshold	0.001

Table 5
RMSE of sample value prediction.

Parameters	1st	2nd	3rd	4th
Plt	8.83×10^{-2}	1.34×10^{-1}	1.46×10^{-1}	1.35×10^{-1}
THDu	5.46×10^{-2}	1.10×10^{-1}	9.76×10^{-2}	7.43×10^{-2}
THDi	4.73×10^{-2}	6.04×10^{-2}	7.02×10^{-2}	9.63×10^{-2}
freq	4.51×10^{-2}	6.06×10^{-2}	7.90×10^{-2}	7.38×10^{-2}

4.2. Testing and results

Table 5 presents the root mean square error (RMSE) [48] for each 1st, 2nd, 3rd and 4th sample value prediction into the future and for each predicted output variable. RMSE can be simply interpreted as

Table 6
Accuracy of the PQ disturbances prediction.

Parameters	Total disturbances [#]	Predicted disturbances [#]	Predicted disturbances [%]
Freq (50 Hz ± 2%)	165	104.4	63.27
THDu (8% <)	787	530.2	67.37
THDi (100% <)	674	481	71.36
Plt (1<)	234	143.8	61.45

the amount of error in variable's prediction in its measured units. In our case, it is necessary to mention that all the predicted variables as well as the input variables were normalized in the range [0,1] according to Ref. [48].

$$RMSE = \sqrt{\frac{\sum_{t=1}^{n}(\hat{y}_t - y_t)^2}{n}} \quad (13)$$

It can be assumed that for the 1st prediction sample value, an increase in the error will be higher than in the 4th — see Table 5.

The best result was obtained in predicting all the PQ-parameters on the 1st sample value. All of them obtained RMSE below 10^{-1} (*freq* — 4.51×10^{-2}, *THDu* — 5.46×10^{-2}, *THDi* — 4.73×10^{-2}, *Plt* — 8.83×10^{-2}), which is very satisfactory considering the fact that it reflects the forecasting error on the entire previously normalized training dataset. The regression error increases when the time scale of forecasting gets longer. This phenomenon is also logical because with a longer forecasted time scale, the relevancies also lowered, which implied the presence of a higher error rate (in forecasting the 4th observation, RMSE was almost double: *freq* — 7.38×10^{-2}, *THDu* — 7.43×10^{-2}, *THDi* — 9.63×10^{-2}, *Plt* — 1.35×10^{-1}). The values of RMSE were considered in further testing as tolerance values for PQ-disturbance detection, which helps to increase the protection of the system with an accuracy over 60 % (see Table 6).

4.3. Optimization of PQ parameters using the developed algorithm

The forecasting model, as we can see in the previous section, did not render a 100%-accurate prediction. This makes us apply its averaged error as the threshold value that works as a disadvantage against all the PQPs' values. This assumption leads to a higher security of the PQ support. The entire block diagram of ADSM, including predictor's integration, is introduced in Fig. 1. ADSM is responsible for the optimization of the consumption structure. The evaluation of the above mentioned optimization is realized in the next step and while the power quality parameters are within the requested limits/range, ADSM works in the next step with the same adjustments until the PQ parameters are in limits.

An example of ADSM including PQPO tools for the tested experimental platform of the Off-Grid system is shown in Fig. 1 and Fig. 3. Fig. 3 is a scenario of several iteration steps for a predominantly cloudy day with variable cloudiness and a variable electric power output from PV_1 and PV_2.

The energy demand controlling mechanism runs in schedule and each of its executions follows the simple steps below:

- At the beginning the process loads the rules of appliance switching and user's adjustments (2). These rules are transformed into the plan of energy demand for the nearest 24 h (3). The estimated energy consumption is computed according to this plan (see 58% in Fig. 4).
- The next step of ADSM loads the energy generation forecast (see 55% in Fig. 4) and state of the storage device — see module (4) in Fig. 4. The percentage expression of electric energy is related to the nominal power in the Off-Grid and individual time step. The nominal power in the Off-Grid system was defined to 5 kW and corresponds to the output power from SI (see Fig. 1).
- ADSM compares the values of the energy consumption and energy generation (6). In our example in Fig. 4, there is a visible deficit of energy (7%) in the first iteration.
- The next phase predicts the PQ parameters (*Δfreq*, *THDi*, *THDu*, *Pst*, *Plt*) as you can see in Fig. 4 (the *Δfreq* is a percentage variation from nominal value 50 Hz). The PQPO module (7) collects information about the actual and predicted PQ parameters.
- The PQ parameters are not in a requested interval (*Δfreq*) and PQPO (7) returns this information to ADSM. Next, ADSM proposes a load shift in the schedule of appliances (2) with the lowest priority (8). In our model example, ADSM proposes replacing the washer 10 min ahead and the optimization process starts a new iteration.

These steps are repeated multiple times until there is a satisfactory amount and quality of the energy for the optimized plan. When the plan modification proposed by a low amount of energy replaces the modification proposed by a low quality of energy, the process stops and the modification proposed by the amount of energy gets a higher priority.

In our model example, ADSM achieves the second iteration (Fig. 4). Due to rescheduling one appliance, the energy generation is higher than the energy consumption (23%). On the other hand, PQPO returns information about the PQ parameters that are out of the requested range (*Δfreq*) within this second iteration (see the second row in Fig. 4). This PQ parameter imbalance was caused by unloading of the Off-Grid system. In this case, the Off-Grid system was supplied directly from PV_1 and PV_2 over the inverters (by-pass system, PVI in Fig. 1). There, PVI is loaded only to 32% (the total output power from inverter is about 1.6 kW) and the frequency is over the limit (*Δfreq* = 0.1 Hz). Therefore, the third iteration must follow (see the third row in Fig. 4).

ADSM proposes the next load shift that will reschedule the washer 30 min ahead. After this ADSM's action, the energy is sufficient for the Off-Grid supply within the third iteration (surplus energy is 3%). PVI is better loaded (about 52%; the total output power from inverter is about 2.6 kW) due to the increase in the whole consumption (washer 1.3 kW + air conditioning 1.3 kW). PQPO returns the information about the PQ parameters, where *Δfreq*, *Pst* and *Plt* are within the limits. However, the PQ parameters *THDi* and *THDu* exceeded the requested limits. This excess was caused by the interference of PVI and air-conditioning inverter. So, the fourth iteration must be realized.

ADSM proposes replacing the washer 30 min ahead (see the fourth row in Fig. 4). The surplus of electric energy is the same as in the third iteration. However, this time the Off-Grid system is not directly supplied from PV_1 and PV_2 using PVI (when no energy from battery bank is needed), but the Off-Grid system is supplied from the battery supply over the Off-Grid converter — SI in Fig. 1 (the energy from PVI only is not sufficient to cover the energy demand). In this case, the short-circuit power is increased (doubled in comparison with the previous case).

The PQ parameters are in the requested limit, the optimized plan is saved (10) and ADSM can switch the selected appliances (11), i.e. the management process is finished.

Via the PQP optimization it is possible to ensure a safe and reliable operation of the entire energy platform. In Ref. [49] the authors

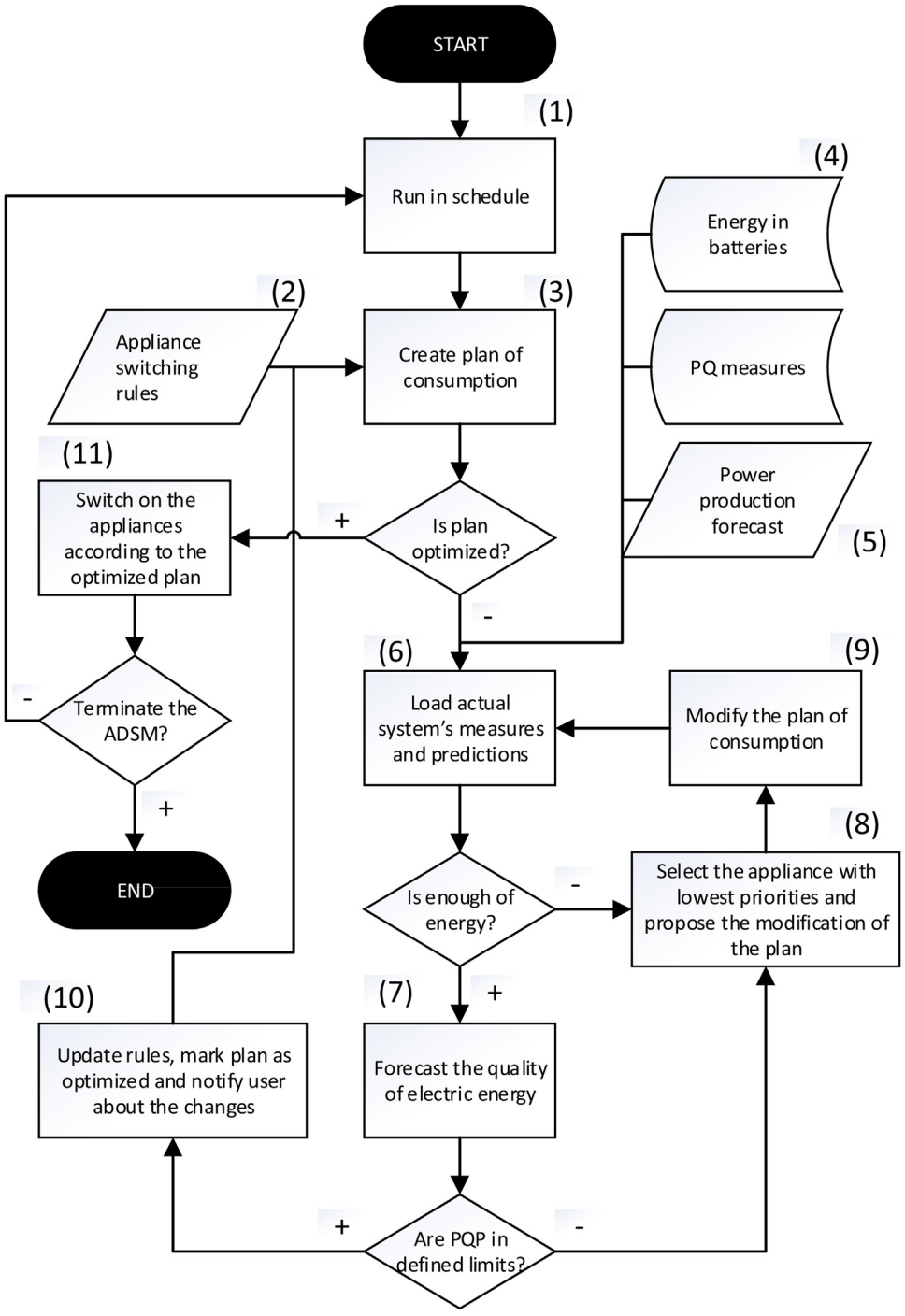

Fig. 3. UML diagram of the optimization process.

clearly demonstrate that the power quality parameters influence the reliability of operation. Next, the cost of poor power quality may be high and this problem may further aggravate in the future [50]. Extreme compliance of PQP is required, for instance, in hospital environments with devices that maintain and monitor vital human functions.

Other important fields of power quality impact are as follows:

- the accuracy of movement of Computer Numeric Control Machines vs voltage drop/frequency,
- the inception of parasitic torque of rotating machines vs frequency changes and flicker severity
- changes in the luminous flux of luminous sources vs flicker severity,
- increasing additional losses and warming of rotating machines vs total harmonic distortion

Table 6 summarizes the fact that the forecasting model was able to avoid more than 60% of the PQ disturbances on our dataset. These events were counted during CV of the PQ forecasting model and averaged across all the CV's executions. The results imply that PQ parameter forecasting and subsequent PQPO are necessary. PQPO reduces the risk of damage in appliances and also utilizes available energy in an optimal manner.

Iteration	Progress of Total Consumption	Energy Production	Max. Consumption	PQP's (max value) Δfreq	THDi	THDu	Plt	Pst	Action
1.	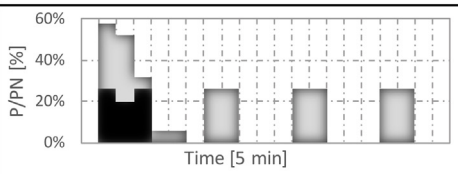	55%	58%	0.1 Hz	15%	3.55%	0.81	1.24	replace washer 10 minutes ahead
2.	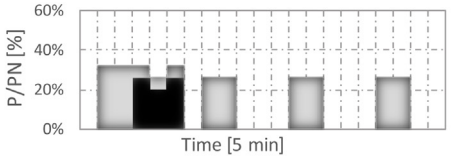	55%	32%	0.1 Hz	15%	4.80%	0.81	1.24	replace washer 10 minutes ahead
3.	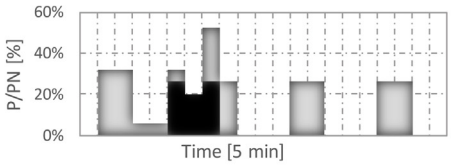	55%	52%	0.05Hz	60%	9.65%	1.4	1.36	replace washer 10 minutes ahead
4.	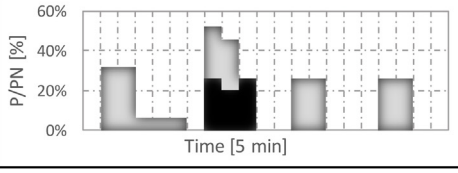	55%	52%	0.05Hz	17%	3.10%	0.91	1.22	no action

Fig. 4. Values of monitored variables during PQPO iterations.

The computational complexity of the entire optimization algorithm (Fig. 4) relies on the number of appliances contained in the optimized consumption plan. Most of the parts of the algorithm work separately and are able to provide pre-computed data (power production forecast, PQ measures, and the amount of energy in batteries). Other parts of the algorithm need some computational effort. The PQ forecasting based on trained SVR has a linear complexity and varies only in the dimensionality of the input data and chosen kernel function. The part of the algorithm that switches the appliances according to their adjusted priority further checks if the amount of requested energy may be fulfilled, it has a brute-force character and its complexity is close to exponential. In case of a lower number of appliances with a lower priority (<100 in average household), the entire optimization algorithm can work reasonably fast on average computational resources.

The success-rate of our approach in avoiding the PQ disturbances can vary in multiple factors, which brings a multi-criteria optimization problem into the model. We can define such criteria from nationally defined limits (IEEE, EN, IEC, etc). On the other hand, the regression errors (residuals) may be taken as tolerance in fine-tuning of the final protection approach. This way, we can adjust the model to react more strictly even when it does not face a real PQ issue, but only a potential one.

5. Conclusion

This paper presents a novel approach to a PQ parameter optimization as an integral part of Active Demand Side Management in AC coupling Off-Grid systems. The values of PQ parameters may be forecasted using artificial intelligence methods, namely support vector regression, and kept in defined limits using this PQPO tool. The developed PQPO algorithm is able to intelligently reschedule the appliances used in the Off-Grid system with regard to their priority and therefore optimizes the consumption process during the day.

In on-grid systems the short-circuit power ranges around 100 kVA and the consumption of electric energy by different users is characteristic of certain regularity levels according to the day load type diagrams. In such systems, even with the supply of energy from a photovoltaic power plant, the variability of a power quality parameter may be predicted much easily, and the prediction success rate ranges from 85% in a group of parameters (*freq* AND *Pst* AND *THDi* OR *THDu*) to 95% in one selected parameter.

However, this article deals with predicting the power quality parameters in the systems that are independent on the power supply from the grid, the so-called Off-Grid Systems, where the conditions differ. In such systems, we need to consider the following: (a) the short-circuit power is slightly higher than the Sunny Island (SI) inverter output, (b) the value of the short-circuit power is highly variable and depends on the operation characteristics of the discrete sources and system configuration that changes several times during one calculation step, i.e. several times per minute, (c) the power quality parameters are directly influenced by the character of the different household appliances, both as for the output profile as well as the internal connection of semiconductor components that interact with the conversion elements (MPPT regulator, SI). Therefore, we claim that the obtained 72% prediction success rate is very good and sufficient to optimize the household appliance plan.

The proposed algorithm gives a satisfactory performance in case of few ticks ahead forecasting. The ticks represent median values of the previous 15 min, which decreases the uncertainty and noise of the time series. Our future work aims to create predictions for lower time-framed data, which will bring more relevant information for ADSM.

The major responsibility of PQPO is to avoid the upcoming PQ disturbance. Our solution presents satisfactory performance in this respect, which is going to be continuously refined during our future work.

Acknowledgements

This research was conducted within the framework of the project TUCENET Sustainable Development of Centre ENET LO1404, Students Grant Competition project reg. no. SP2017/157, SP2017/159 and project CZ.1.05/2.1.00/19.0389. Next, we would like to thank for language corrections to Ms. Alena Kasparkova, Ph.D.

References

[1] S. Mišák, J. Stuchlý, J. Platoš, P. Kromer, A heuristic approach to Active Demand Side Management in Off-Grid systems operated in a Smart-Grid environment, Energy Build. 96 (2015) 272–284.
[2] J.A. Martinez, J. Martin-Arnedo, Tools for analysis and design of distributed resources—part I: tools for feasibility studies, IEEE Trans. Power Del. (July) (2011) 1643–1652.
[3] Sara Lumbreras, Andrés Ramos, The new challenges to transmission expansion planning. Survey of recent practice and literature review, Electr. Power Syst. Res. 134 (2016) 19–29.
[4] W. Al-Saedi, S.W. Lachowicz, D. Hababi, O. Bass, Power quality enhancement in autonomous microgrid operation using Particle Swarm Optimization, Int. J. Electr. Power Energy Syst. 42 (1) (2012) 139–149.
[5] O. Ipinnimo, S. Chowdhury, S.P. Chowdhury, J. Mitra, review of voltage dip mitigation techniques with distributed generation in electricity networks, Electr. Power Syst. Res. 103 (2013) 28–36.
[6] D. Ferreira Danton, José M. de Seixas, S. Cerqueira Augusto, A. Duque Carlos, H.J.Bollen Math, F.Ribeiro Paulo, A new power quality deviation index based on principal curves, Electr. Power Syst. Res. 125 (2015) 8–14.
[7] W.G. Morsi, M.E. El-Hawary, Power quality evaluation in smart Grids considering modern distortion in electric power systems, Electr. Power Syst. Res. 81 (2011) 1117–1123.
[8] A.Q. Lawey, T.E.H. El-Gorashi, J.M.H. Elmirghani, Renewable energy in distributed energy efficient content delivery clouds, IEEE International Conference on Communications (ICC) (2015).
[9] N.M.Silva Elson, B.Rodrigues Anselmo, a. Maria da Guia da Silv, Stochastic assessment of the impact of photovoltaic distributed generation on the power quality indices of distribution networks, Electr. Power Syst. Res. 135 (2016) 59–67.
[10] S. Conti, R.S. Agatino, Modelling of microgrid-renewable generators accounting for power-output correlation, IEEE Trans. Power Deliv. 28 (2013) 2124–2133.
[11] M. Singh, V. Khadkikar, A. Chandra, R.K. Varma, Grid interconnection of renewable energy sources at the distribution level with power-quality improvement features, IEEE Trans. Power Deliv. 26 (1) (2011) 307–315.
[12] J. Liu, C.H. Hsiao-Dong, Maximizing available delivery capability of unbalanced distribution networks for high penetration of distributed generators, IEEE Trans. Power Deliv. (2014) 1–5.
[13] Y. Hong, L. Ruo-Chen, Optimal sizing of hybrid wind/pv/diesel generation in a stand-alone power system using Markov-based genetic algorithm, IEEE Trans. Power Deliv. 27 (2) (2012) 640–647.
[14] S.F. Abdelsamad, W.G. Morsi, T.S. Sidhu, Optimal secondary distribution system design considering plug-in electric vehicles, Electr. Power Syst. Res. 130 (2016) 266–276.
[15] E. Ozan, P.G. Nikolaos, P.S.C. Joao, Overview of insular power systems under increasing penetration of renewable energy sources: opportunities and challenges, Renew. Sustain. Energy Rev. 52 (2015) 333–346.
[16] S.N. Afifi, M.K. Darwish, Impact of hybrid renewable energy systems on short circuit levels in distribution networks, 49th International Universities Power Engineering Conference (UPEC) (2014).
[17] J.C. Das, Power System Analysis Short-circuit Load Flow and Harmonics, 2nd ed., CRC Press, FL, 2012, ISBN 14-398-2080-5.
[18] Hojabrin Mojgan, Arash Toudeshki, Power quality consideration for Off-Grid renewable energy systems, Energy Power Eng. 5 (2013) 377–383.
[19] S. Mišák, J. Stuchlý, J. Vramba, T. Vantuch, D. Seidl, A novel approach to adaptive active relay protection system in single phase AC coupling Off-Grid systems, Electr. Power Syst. Res. 131 (2016) 159–167.
[20] Ko Hee-Sang, Y. Lee Kwang, Kang Min-Jae, Kim Ho-Chan, Power quality control of an autonomous wind–diesel power system based on hybrid intelligent controller, Neural Netw. 21 (10) (2008) 1439–1446.
[21] A. Moreno-Munoz, J.J.G. de-la-Rosa, M.A. Lopez-Rodriguez, J.M. Flores-Arias, F.J. Bellido-Outerino, M. Ruiz-de-Adana, Improvement of power quality using distributed generation, Int. J. Electr. Power Energy Syst. 32 (10) (2010) 1069–1076.
[22] Shuyong Chen, Ningchao Gao, Hong Shen, Yusheng Quan, Cong Wang, Lin Zhu, Jianwei Liu, Affect analysis of power grid energy quality for coastal wind power access, Energy Procedia 12 (2011) 752–760.
[23] Hermes M.G.C. Branco, Mário Oleskovicz, Alexandre C.B. Delbem, Denis V. Coury, Raphael P.M. Silva, Optimized allocation of power quality monitors in transmission systems: a multiobjective approach, Int. J. Electr. Power Energy Syst. 64 (2015) 156–166.
[24] C. Buccella, C. Cecati, H. Latafat, Digital control of power converters—a survey, IEEE Trans. Ind. Inform. 8 (3) (2012) 437–447.
[25] T.E. Raptis, G.A. Vokas, P.A. Langouranis, S.D. Kaminaris, Total power quality index for electrical networks using neural networks, Energy Procedia 74 (2015) 1499–1507.
[26] D. De Yong, S. Bhowmik, F. Magnago, An effective power quality classifier using wavelet transform and support vector machines, Expert Syst. Appl. 42 (15–16) (2015) 6075–6081.
[27] G.W. Chang, H.J. Lu, Forecasting flicker severity by grey predictor, IEEE Trans. Power Deliv. 27 (4) (2012) 2428–2430.
[28] Diego Piasson, André A.P. Bíscaro, Fábio B. Leão, José Roberto, Sanches Mantovani, A new approach for reliability-centered maintenance programs in electric power distribution systems based on a multiobjective genetic algorithm, Electr. Power Syst. Res. 137 (2016) 41–50.
[29] Mohammad Valipour, Optimization of neural networks for precipitation analysis in a humid region to detect drought and wet year alarms, Meteorol. Appl. 23.1 (2016) 91–100.
[30] Sebastian Basterrech, Lukas Prokop, Tomas Burianek, Stanislav Misak, Optimal design of neural tree for solar power prediction, Proccedings of the 2014 15th International Scientific Conference on Electric Power Engineering (EPE). IEEE (2014).
[31] O.P. Mahela, A.G. Shaik, N. Gupta, A critical review of detection and classification of power quality events, Renew. Sustain. Energy Rev. 41 (2015) 495–505.
[32] M.K. Saini, R. Kapoor, Classification of power quality events — a review, Int. J. Electr. Power Energy Syst. 43 (2012) 11–19.
[33] SMA Solar Technology AG. Sunny Island 3324/4248 User Manual, Available from: http://www.rpc.com.au/pdf/SMA_SI3324_4248_user_manual.pdf.
[34] H. Almuallim, T.G. Dietterich, Learning with many irrelevant features, Proceedings of the Ninth National Conference on Artificial Intelligence, AAAI Press (1991) 547–552.
[35] D.J.C. MacKay, Information Theory, Inference & Learning Algorithms, Cambridge University Press, New York, NY, USA, 2002.
[36] C.W.J. Granger, Investigating causal relations by econometric models and cross-spectral methods, Econometrica 37 (3) (1969) 424–438.
[37] A. Kraskov, H. Stögbauer, P. Grassberger, Estimating mutual information, Phys. Rev. 69 (6) (2004) 66–138.
[38] Gauthier Doquire, Michel Verleysen, A Comparison of Multivariate Mutual Information Estimators for Feature Selection. ICPRAM (1), 2012.
[39] Ratko Grbić, Dražen Slišković, Petr Kadlec, Adaptive soft sensor for online prediction and process monitoring based on a mixture of Gaussian process models, Comput. Chem. Eng. 58 (2013) 84–97.
[40] Vincent Michel, Cécilia Damon, Bertrand Thirion, Mutual information-based feature selection enhances fMRI brain activity classification, 5th IEEE International Symposium on Biomedical Imaging: From Nano to Macro. IEEE (2008).
[41] S. Misak, Tomas Burianek, Jindrich Stuchly, Solar power production forecasting based on recurrent neural network, Afro-European Conference for Industrial Advancement Advances in Intelligent Systems and Computing (2016).
[42] Vladimir Naumovich Vapnik, Vlamimir Vapnik, Statistical Learning Theory, Wiley, New York, 1998, pp. 1.
[43] A.A. Yusuff, et al., Fault location in a series compensated transmission line based on wavelet packet decomposition and support vector regression, Electr. Power Syst. Res. 81 (7) (2011) 1258–1265.
[44] Yukimasa Kaneda, Hiroshi Mineno, Sliding window-based support vector regression for predicting micrometeorological data, Expert Syst. Appl. 59 (2016) 217–225.
[45] Dimitri P. Bertsekas, Nonlinear Programming, Athena scientific, Belmont, 1999.
[46] Yassi Maryam, Mohammad Hossein Moattar, Optimal SVM parameters estimation using chaotic accelerated particle swarm optimization for genetic data classification, Technology, Communication and Knowledge (ICTCK), International Congress on IEEE (2014).
[47] J. Kennedy, The particle swarm: social adaptation of knowledge, Evolutionary Computation, IEEE International Conference on IEEE (1997) 303–308.
[48] R. Kohavi, et al., A study of cross-validation and bootstrap for accuracy estimation and model selection, IJCAI 14 (1995) 1137–1145.
[49] A. Honrubia-Escribano, E. Gómez-Lázaro, A. Molina-Garcia, S. Martin-Martinez, Load influence on the response of AC-contactors under power quality disturbances, Int. J. Electr. Power Energy Syst. 63 (2014) 846–854.
[50] Judith Res, Jack Herring, Michał Sopocko, Paul Dempsey, Sara Armstrong, Survey on demand side sensitivity to power quality in Ireland, Int. J. Electr. Power Energy Syst. 83 (2016) 495–504.